Thermonuclear reaction rate of ^{57}Cu$(p,\gamma)^{58}$Zn in the *rp* process

M. Zhang [1,2] X. Xu [1,2,*] Y. M. Xing,[1,2,†] and S. Q. Hou [1,2,‡]

[1]*CAS Key Laboratory of High Precision Nuclear Spectroscopy, Institute of Modern Physics, Chinese Academy of Sciences, Lanzhou 730000, China*

[2]*School of Nuclear Science and Technology, University of Chinese Academy of Sciences, Beijing 100049, China*

(Received 11 October 2023; accepted 13 March 2024; published 2 April 2024)

The mass of neutron-deficient nuclide ^{58}Zn has been directly measured by using $B\rho$-defined isochronous mass spectrometry, resulting in a more precise proton separation energy of $S_p(^{58}\mathrm{Zn}) = 2227(36)$ keV. With this new S_p value, the thermonuclear rate of the ^{57}Cu$(p,\gamma)^{58}$Zn reaction has been re-evaluated to be higher than the most recently published rate by a factor of up to 3 in the temperature range of 0.2 GK $\lesssim T \lesssim$ 1.5 GK. The new rate is used to investigate its astrophysical impact via one-zone post-processing type-I x-ray burst calculations. It shows that the updated rate and new $S_p(^{58}\mathrm{Zn})$ value result in noticeable abundance variations for nuclei with $A = 56$–59 and a reduction in $A = 57$ abundance by up to 20.7%, compared with the results using the recently published rate.

DOI: 10.1103/PhysRevC.109.045802

I. INTRODUCTION

Type-I x-ray bursts (XRBs) are the most frequently observed thermonuclear explosions in the galaxy [1–3]. The prevailing scenario proposed that XRBs could be powered by thermonuclear runaways on the accreted envelopes of neutron stars in binary systems [4–6]. The high temperature and densities, created by accreted material on the neutron star surface, may transform the envelope, initially enriched in H and He, to matter enriched in heavier species via the αp process and the rapid proton capture process (rp process) [7–11]. The rp process is a sequence of proton captures and subsequent β^+ decays. The amount of energy released can be directly observed as an x-ray burst and the time scale of the thermal runaway ranges between 10 s and several minutes [2]. In order to quantitatively understand the shape of the burst light curve and the composition of the neutron star crust, detailed nuclear reaction network calculations are required. Of particular importance to the x-ray burst models are the nuclear masses of neutron-deficient nuclides involved in the rp process [9,12,13].

The so-called waiting points in the rp process are essential to qualitatively understand the extended tails of the light curves. A waiting point is a nucleus with the low or even negative proton-capture Q values and relatively long β-decay half-lives, thus hindering the reaction flow towards heavier elements. The effective lifetimes of waiting points are needed to interpret the XRBs observations and predict the composition of burst ashes. The doubly magic nucleus ^{56}Ni is identified as one of the most interesting rp-process waiting points. With a small ^{56}Ni(p,γ) reaction Q value of 690.3(4) keV [14] and an hours-long decay lifetime under typical x-ray burst conditions [7,9,15], ^{56}Ni was historically thought to be the end point of the rp process [7]. However, it was later shown that the rp process can proceed beyond ^{56}Ni to higher masses [16,17]. The reaction flow passing ^{56}Ni is mainly through ^{56}Ni$(p,\gamma)^{57}$Cu$(p,\gamma)^{58}$Zn [18], see Fig. 1. At present, all the quantities related to the effective lifetime of ^{56}Ni under typical x-ray burst conditions have been constrained experimentally. Up to now, the largest uncertainty concerning the ^{56}Ni waiting point is mainly originated from the uncertainty of ^{57}Cu$(p,\gamma)^{58}$Zn reaction rate [20].

The ^{57}Cu$(p,\gamma)^{58}$Zn reaction determines the stellar effective lifetime of ^{56}Ni at high temperature (0.7–1.4 GK) when ^{56}Ni and ^{57}Cu are in (p,γ)-(γ,p) equilibrium [18]. Given the significant impact of this reaction on the rp process, Forstner *et al.* [18] predicted the properties of the ^{58}Zn resonance energy levels based on shell model calculations and constructed the ^{57}Cu$(p,\gamma)^{58}$Zn reaction rate, concluding that it is not the ^{57}Cu$(p,\gamma)^{58}$Zn reaction rate but the ^{58}Zn β^+ decay rate that determines the ^{56}Ni lifetime in the rp process at high temperatures. Later, Langer *et al.* [20] experimentally confirmed some low-lying energy levels of ^{58}Zn, which are dominant resonances contributing to the ^{57}Cu$(p,\gamma)^{58}$Zn reaction rate in the typical rp-process temperature range. These precisely measured energy levels largely reduced the rate uncertainty by up to three orders of magnitude compared to the reaction rate constructed in Ref. [18]. Langer *et al.* [20] claimed that, based on a preliminary calculations with an x-ray burst model, the three orders of magnitude reduction of uncertainty of just this reaction may reduce the uncertainty in $A = 56$ production by a factor of 10. Recently, Lam *et al.* [21] proposed a possible order of 1^+_1- and 2^+_3-dominant resonance states, which was unconfirmed in Ref. [20], and constrained the resonance energy of the 1^+_2 state based on the shell model calculations

*xuxing@impcas.ac.cn
†xym@impcas.ac.cn
‡sqhou@impcas.ac.cn

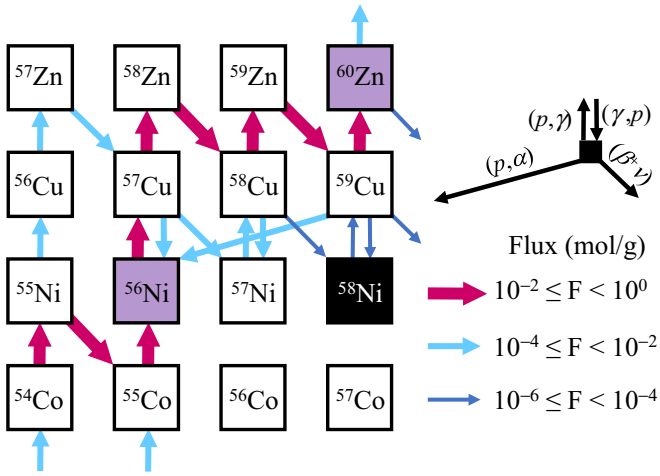

FIG. 1. The rp-process path passing through the ^{56}Ni waiting point. Stable nuclei are represented by black filled squares, and waiting points are shown in purple filled squares. The figure is obtained from the calculation using NUCNET code [19].

and the isobaric-multiplet-mass equation. As a result, the new reaction rate is lower than the rate in Ref. [20] by a factor of 2, and the new rate coupled with the latest ^{56}Ni(p,γ) rate [22] can strongly influence the burst ash composition found from the x-ray burst model calculation [21].

So far the uncertainty of ^{57}Cu$(p,\gamma)^{58}$Zn reaction rate is dominated by the 50 keV uncertainty of the proton separation energy (S_p) of ^{58}Zn propagated from its mass [20,21]. The current mass excess value ME(^{58}Zn) = −42300(50) keV tabulated in AME2020 [14] was determined nearly 40 years ago by measuring the Q value of a double charge-exchange reaction ^{58}Ni$(\pi^+,\pi^-)^{58}$Zn [23]. Recently, we precisely measured the masses of a series of $T_z = -1$ fp-shell nuclides [24] including ^{58}Zn by using the newly established $B\rho$-defined isochronous mass spectrometry ($B\rho$-IMS) [25,26]. The experiment was conducted at the Cooler Storage Ring of the Heavy Ion Research Facility in Lanzhou (HIRFL-CSR) [27–29], see Ref. [24] for details of the experiment. The new mass excess of ^{58}Zn was determined to be −42248(36) keV, which is 52 keV less bound and more precise than AME2020 value, resulting in a new $S_p(^{58}\text{Zn}) = 2228(36)$ keV. This allows us to reevaluate the thermonuclear reaction rate of ^{57}Cu$(p,\gamma)^{58}$Zn and its influence on the astrophysical rp process.

II. CALCULATION OF STELLAR REACTION RATE

The total thermonuclear proton-capture reaction rate is predominantly determined by summing the contributions from isolated resonances corresponding to unbound compound nuclear states and from the non-resonant direct capture (DC) process. The resonant reaction rate can be calculated from resonance energy E_r and resonance strength $\omega\gamma$ (both in units of MeV) by the well-known narrow resonance formalism [8,18,21,30],

$$N_A\langle\sigma v\rangle_{\text{res}} = 1.54\times10^{11}(\mu T_9)^{-3/2}\sum_{\text{res}}\omega\gamma \times \exp(-11.605E_r/T_9), \quad (1)$$

in units of cm^{3}mol^{-1}s^{-1}, where $\mu = A_pA_T/(A_p+A_T)$ is the reduced mass of the entrance channel in atomic mass units with A_p and A_T being the mass numbers of proton and target nucleus, respectively. T_9 is the temperature in unit of GK. $E_r = E_x - Q$ with E_x and Q being the excitation energy of resonant state and the Q value of the reaction, respectively. The $\omega\gamma$ of an isolated resonance for a (p,γ) reaction is given by

$$\omega\gamma = \frac{2J+1}{(2J_p+1)(2J_T+1)}\frac{\Gamma_p\Gamma_\gamma}{\Gamma_{\text{tot}}}, \quad (2)$$

where J, J_p, and J_T are the spins of the resonant state, proton and the target nucleus, respectively. The total width Γ_{tot} is the sum of the proton-decay width Γ_p and the γ-decay width Γ_γ.

The Γ_p can be expressed in the framework of shell-model formalism as

$$\Gamma_p = \sum_{nlj} C^2S(nlj)\Gamma_{\text{sp}}(nlj), \quad (3)$$

where $\Gamma_{\text{sp}}(nlj)$ is a single-particle width for the capture of a proton with respect to a given (nlj) quantum orbital in a spherically symmetric mean-field potential, while $C^2S(nlj)$ denotes a corresponding spectroscopic factor containing information of the structure of the initial and final states. In this work, the proton widths of the important ^{57}Cu$(p,\gamma)^{58}$Zn resonances are calculated following the same procedure as was used in Ref. [21].

The Γ_γ are calculated from electromagnetic reduced transition probabilities $B(\Omega L; J_i \to J_f)$ (Ω stands for electric or magnetic), which carry the nuclear structure information of the resonance states J_i and the final bound states J_f. The corresponding γ-decay widths for the most contributed transitions ($M1$ and $E2$) can be expressed within the framework of shell model as [30]

$$\Gamma_{E2} = 8.13\times10^{-7}E_\gamma^5B(E2) \quad (4)$$

and

$$\Gamma_{M1} = 1.16\times10^{-2}E_\gamma^3B(M1), \quad (5)$$

both are in units of eV, while $B(E2)$, $B(M1)$, and E_γ are in units of e^2fm^4, μ_N^2, and MeV, respectively. The total electromagnetic decay width is obtained by summing all partial decay widths for a given initial state.

The resonant parameters of six dominant resonances listed in Ref. [21] are recalculated in the framework of the KSHELL code [31] based on a full fp-model space with the GXPF1a Hamiltonian [32], and summarized in Table I.

The direct-capture rate can be approximately calculated by the equation [18] in a form of

$$N_A\langle\sigma v\rangle_{\text{DC}} = 7.833\times10^9\left(\frac{Z_pZ_T}{\mu T_9^2}\right)^{1/3}S(E_0) \times \exp\left[-4.249\left(\frac{\mu Z_p^2Z_T^2}{T_9^2}\right)^{1/3}\right] \quad (6)$$

using an astrophysical S factor of $S(E_0) = 0.0575$ MeV b [20], with E_0 being the position of the Gamow peak corresponding to the effective bombarding energy range of stellar

TABLE I. Parameters for the present ^{57}Cu$(p,\gamma)^{58}$Zn reaction rate calculation.

J_i^π	E_x (MeV)	E_r (MeV)	$C^2S_{7/2}$ ($l=3$)	$C^2S_{3/2}$ ($l=1$)	$C^2S_{5/2}$ ($l=3$)	$C^2S_{1/2}$ ($l=1$)	Γ_γ (eV)	Γ_p (eV)	$\omega\gamma$ (eV)
2_2^+	2.609(6)	0.381	0.0027	0.5776	0.0063	0.1144	9.034×10^{-3}	6.024×10^{-9}	3.765×10^{-9}
1_1^+	2.861(4)	0.633		0.0000	0.6522	0.0867	7.300×10^{-3}	1.792×10^{-4}	6.559×10^{-5}
2_3^+	2.904(5)	0.676	0.0020	0.0131	0.0103	0.1649	5.278×10^{-3}	1.444×10^{-4}	8.785×10^{-5}
2_4^+	3.265(6)	1.037	0.0005	0.1174	0.4953	0.0002	4.131×10^{-3}	3.187×10^{-1}	2.549×10^{-3}
2_5^+	3.605(22)	1.377	0.0012	0.0011	0.0302	0.2498	3.677	5.093	8.645×10^{-3}
1_2^+	3.664(22)	1.436		0.0000	0.1011	0.5980	4.526×10^{-2}	$2.030\times10^{+1}$	1.693×10^{-2}

burning [18]. Equation (6) is in units of cm^{3}mol^{-1}s^{-1}. For the ^{57}Cu$(p,\gamma)^{58}$Zn reaction, the contribution of direct rate is several orders of magnitude lower than the contribution of the dominating resonances throughout XRB related temperature range from 0.1 to 2 GK [18,20,21]. Therefore, the contribution of the direct-capture rate is negligible for the reaction rate of ^{57}Cu$(p,\gamma)^{58}$Zn.

The proton capture rates of main contributing resonances of ^{57}Cu$(p,\gamma)^{58}$Zn reaction determined in this work with updated Γ_p and $S_p(^{58}\text{Zn})$ is presented in the lower panel of Fig. 2. The total ^{57}Cu$(p,\gamma)^{58}$Zn reaction rate is determined by summing up the contributions of all the dominating

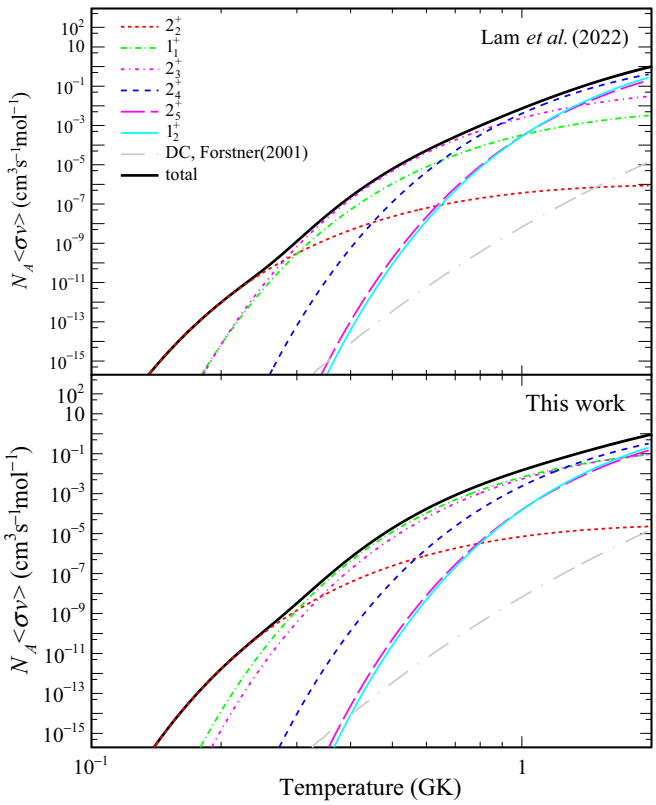

FIG. 2. Thermonuclear reaction rates of ^{57}Cu$(p,\gamma)^{58}$Zn. Upper panel: Lam *et al*. rates [21] reproduced by using the parameters listed in Ref. [21]. The main contributing resonances of proton capture on ground state of ^{57}Cu are indicated as dashed color lines. Lower panel: The reaction rates determined in this work with updated Γ_p and $S_p(^{58}\text{Zn})$.

resonances as well as DC contribution, also plotted in the lower panel of Fig. 2 and tabulated in Table II. The upper panel of Fig. 2 presents the Lam *et al.* rate [21] reproduced by using the parameters listed in Ref. [21].

Figure 3 shows the comparison of our new rate with five different rates [all of them are based on a S_p value of 2.280(50) MeV] for ^{57}Cu$(p,\gamma)^{58}$Zn reaction: (a) the Hauser-Feshbach statistical model rate ths8_v4 available in the Joint Institute for Nuclear Astrophysics (JINA) nuclear reaction rate library (REACLIB) [33,34]; (b) the Hauser-Feshbach statistical model rate rath_v2 in the REACLIB; (c) the wien2 rate [18] recommended by REACLIB; (d) the rate from Langer *et al.* [20]; and (e) the rate from Lam *et al.* [21]. The uncertainties of the present and Lam *et al.* rates are both dominated by the separately adopted Q values. In comparison to the rate by Lam *et al.*, it is seen from Fig. 2 that the resonance contribution of the 1_1^+ state becomes larger with the adoption of the new proton separation energy, finally resulting in an increase of a factor of 1.2-3.2 in total reaction rate over the temperature

TABLE II. Thermonuclear ^{57}Cu$(p,\gamma)^{58}$Zn reaction rate, all the rates are in units of cm^{3}mol^{-1}s^{-1}. The lower and upper limits correspond to the rates when ^{58}Zn mass is shifted 1σ up and down, respectively.

T (GK)	Recommended	Lower limit	Upper limit
0.1	1.18×10^{-21}	1.81×10^{-23}	7.70×10^{-20}
0.2	1.68×10^{-12}	2.08×10^{-13}	1.36×10^{-11}
0.3	3.28×10^{-9}	8.14×10^{-10}	1.32×10^{-8}
0.4	6.37×10^{-7}	2.24×10^{-7}	1.81×10^{-6}
0.5	1.85×10^{-5}	8.03×10^{-6}	4.27×10^{-5}
0.6	1.72×10^{-4}	8.60×10^{-5}	3.46×10^{-4}
0.7	8.38×10^{-4}	4.61×10^{-4}	1.52×10^{-3}
0.8	2.74×10^{-3}	1.62×10^{-3}	4.61×10^{-3}
0.9	6.93×10^{-3}	4.36×10^{-3}	1.10×10^{-2}
1.0	1.48×10^{-2}	9.77×10^{-3}	2.25×10^{-2}
1.1	2.83×10^{-2}	1.94×10^{-2}	4.14×10^{-2}
1.2	4.97×10^{-2}	3.51×10^{-2}	7.05×10^{-2}
1.3	8.21×10^{-2}	5.95×10^{-2}	1.13×10^{-1}
1.4	1.29×10^{-1}	9.56×10^{-2}	1.74×10^{-1}
1.5	1.94×10^{-1}	1.47×10^{-1}	2.56×10^{-1}
1.6	2.81×10^{-1}	2.17×10^{-1}	3.65×10^{-1}
1.7	3.95×10^{-1}	3.09×10^{-1}	5.05×10^{-1}
1.8	5.39×10^{-1}	4.27×10^{-1}	6.80×10^{-1}
1.9	7.16×10^{-1}	5.75×10^{-1}	8.92×10^{-1}
2.0	9.29×10^{-1}	7.54×10^{-1}	1.14×10^{0}

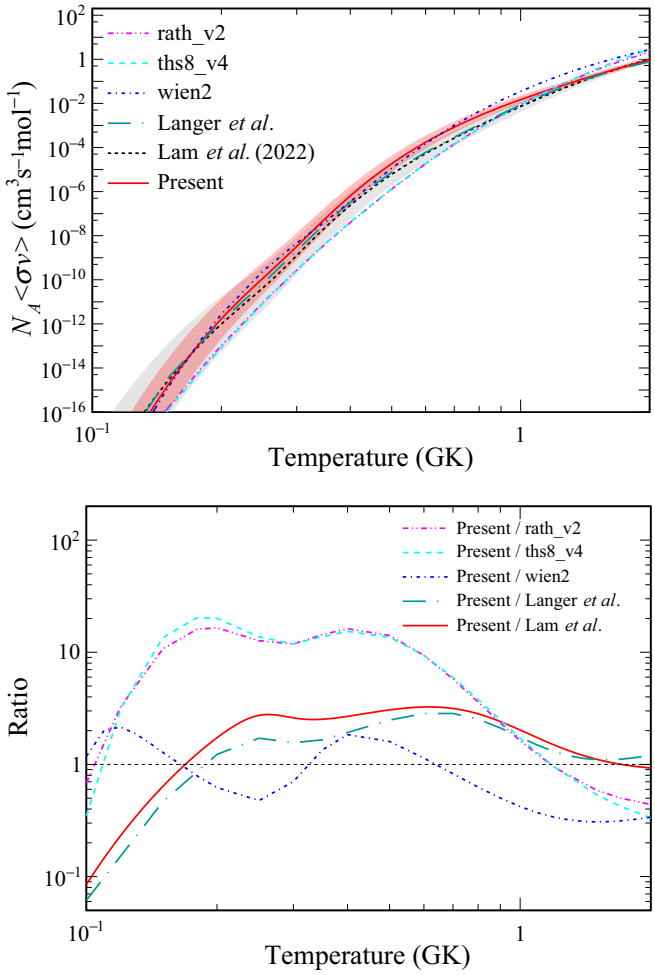

FIG. 3. Comparison of different thermonuclear reaction rate of ^{57}Cu$(p,\gamma)^{58}$Zn. Top panel: Our new rate and five different rates [21,34], see text. The black dashed line and the red solid line represent Lam *et al.* rate [21] and present rate, respectively. The 1σ uncertainties of Lam *et al.* and present rates are indicated by the gray and red zones, respectively. Bottom panel: The ratios of the present rate over other different rates.

range of 0.7-1.4 GK. In the temperature of $T < 0.17$ GK, the decrease of the total rate is mainly owing to the decrease of our new resonant rate of 2^+_2 resonant state, also see Fig. 2. Furthermore, our new rate calculated with the direct mass measurement of ^{58}Zn has smaller uncertainties than the previous ones. Specifically, the reduction of 1σ mass uncertainty from 50 keV to 36 keV, reduces the maximun relative uncertainty from 129% in Lam *et al.* rate to 82% in the present rate over the temperature range of interest for X-ray bursts, as show in top panel of Fig. 3.

The ratios of the present rate over other different rates are shown in the bottom panel of Fig. 3. The statistical model rates ths8_v4 and rath_v2 are very similar in the temperature range of 0.1-2 GK, and both of them deviate considerably from our new rate over the entire temperature region of interest. This shows that the Hauser-Feshbach statistical model rates may be not suitable for this reaction for the low level densities of low-lying excited states of ^{58}Zn. The wien2 rate

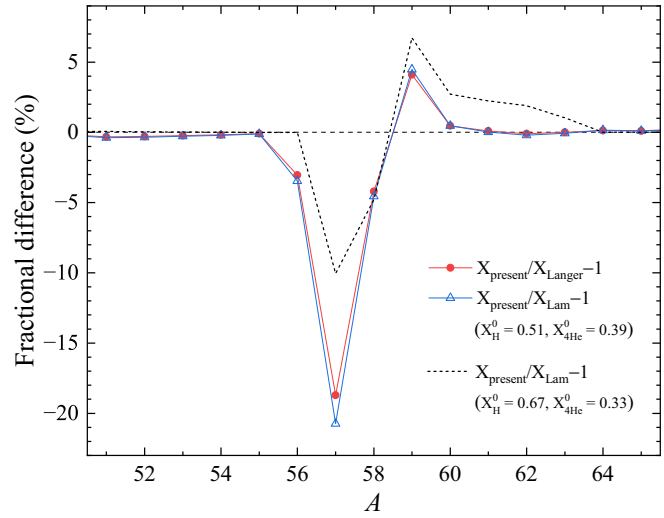

FIG. 4. Fractional difference of abundance by mass number of this work (present) compared to those using Langer *et al.* rate (red filled circles) and Lam *et al.* rate (blue open triangles). The black dashed line represents the result with initial mass fractions from Ref. [16].

[18] recommended by REACLIB shows an oscillation behavior around our new rate in the temperature range of $T < 0.65$ GK, and it is higher than our new rate by up to a factor of 3 in the high temperature range of interest. With a smaller S_p value extracted from the newly determined ^{58}Zn mass [24], the present rate is higher than Lam *et al.* and Langer *et al.* rates by up to a factor of 3 in the temperature range of 0.2 GK $\lesssim T \lesssim$ 1.5 GK.

III. ASTROPHYSICAL IMPLICATIONS

The astrophysical impact of the present ^{57}Cu$(p,\gamma)^{58}$Zn reaction rate is investigated in the framework of one-zone XRB models. We performed a series of post-processing calculations to explore the influence of our new rate and new mass value of ^{58}Zn, as well as the rates from Refs. [18,20,21] and ^{58}Zn mass from AME2020 [14], on the abundances of XRB ashes. The reverse rates are obtained through the principle of detailed balance and are sensitive to the Q values of the forward reactions [35–37]. All calculations are performed by using the one-zone post-processing nucleosynthesis code NUCNET [19]. The initial hydrogen and helium mass fractions of the accreted material are $X^0_{\rm H} = 0.51$ and $X^0_{^4{\rm He}} = 0.39$. Ignition takes place at a temperature of 0.386 GK and a density of 3.4×10^5 g/cm^3. These ignition conditions were chosen to produce light curves and final compositions to most closely resemble those of multizone models and the burst reaches a peak temperature of 1.2 GK, as demonstrated in Ref. [3].

The fractional differences of abundances, as a function of mass number A, of burst ashes calculated by using four different forward and reverse rates of ^{57}Cu$(p,\gamma)^{58}$Zn are shown in Fig. 4. To illustrate the influence of different initial compositions on the final abundances, we also performed a calculation using the initial mass fractions of $X^0_{\rm H} = 0.67$ and

$X^0_{^4\mathrm{He}} = 0.33$, taken from Ref. [16]. The pattern of fractional difference using initial mass fractions from Ref. [16] (Black dash line in Fig. 4) is similar to the result of using those from Ref. [3] (blue open triangles in Fig. 4). We also notice that comparing with the result using Cyburt *et al.* initial mass fractions [3], a noticeable increase around the $A = 60$ mass region is observed for using initial mass fractions from Ref. [16]. This is because the accreted material with a higher proportion of protons will be more helpful in the synthesis of heavier elements. In the following, the results with initial mass fractions of $X^0_{\mathrm{H}} = 0.51$ and $X^0_{^4\mathrm{He}} = 0.39$ are discussed in detail.

The significant differences in elemental abundances of burst ashes can be seen for $A = 56$–59 mass range. In general, for the $A = 56$–59 mass range, the mass fractions using Lam *et al.* [21] and Langer *et al.* [20] rates deviate slightly from each other, both are significantly different from the results obtained by using our new rate. This is reasonable if one carefully inspects the reaction rate ratio shown in Fig. 3, especially in the temperature range of higher than 0.386 GK. As shown, the Lam *et al.* and the Langer *et al.* rates are relatively similar and are always lower than the present rate in the temperature range of interest. The present higher rate contributes to an enhancement of the reaction flow to ^{58}Zn from proton capture of ^{57}Cu, resulting in more abundance of ^{58}Zn and less abundance of ^{57}Cu and subsequent ^{57}Ni. So in Fig. 4, an apparent reduction of abundance at $A = 57$ is observed, by about 20%. The abundance of $A = 58$ is also reduced by ∼5%. This is actually a comprehensive effect of the increased net flow of $^{57}\mathrm{Cu}(p,\gamma)^{58}\mathrm{Zn}$ and the decreased net flow of $^{57}\mathrm{Ni}(p,\gamma)^{58}\mathrm{Cu}$. During rp process, the increased ^{58}Zn by $^{57}\mathrm{Cu}(p,\gamma)^{58}\mathrm{Zn}$ is promptly transformed into heavier isotopes through the main reaction channels (the paths marked in red arrow in Fig. 1). In other words, the increase of $^{57}\mathrm{Cu}(p,\gamma)^{58}\mathrm{Zn}$ rate is able to intensify the material accumulation on long lifetimes nuclei ^{59}Cu and ^{60}Zn. So the actual production of ^{58}Cu will be reduced relative to the case of using original smaller $^{57}\mathrm{Cu}(p,\gamma)^{58}\mathrm{Zn}$ rate, finally resulting in the reduction in ^{58}Ni (β-decay daughter of ^{58}Cu) production. That is the reason why the yields of nuclei with $A = 58$ decrease while those of $A = 59, 60$ increase.

IV. SUMMARY

We recalculated the stellar thermonuclear rate of the $^{57}\mathrm{Cu}(p,\gamma)^{58}\mathrm{Zn}$ reaction using the new mass value of ^{58}Zn measured most recently by $B\rho$-IMS. Our new rate is generally higher than other rates found in literature. Specifically, it is higher than the most recent published rate (Lam *et al.* rate [21]) by a factor of up to 3 in the temperature range of interest, showing a speed-up of rp process flow at waiting point nucleus ^{56}Ni.

To investigate the impact of our new rate on x-ray burst, we conducted the astrophysical network calculations using the one-zone x-ray burst model. The result showed that the abundances of burst ashes are dramatically influenced by our new reaction rate, the mass fractions decrease in ashes of $A = 56$ and 57 by up to 20% and increase slightly around the $A = 59$ mass region.

Although the uncertainty of our rate is smaller than previous ones, it is still dominated by the 36 keV uncertainty of ^{58}Zn mass value. Thus, more precise mass measurement of ^{58}Zn is desired to deduce the uncertainty. Nonetheless, we still recommend that the updated $^{57}\mathrm{Cu}(p,\gamma)^{58}\mathrm{Zn}$ reaction rate using more precise $S_p(^{58}\mathrm{Zn})$ value should be incorporated in future astrophysical network calculations.

ACKNOWLEDGMENTS

The authors acknowledge Dr. Liyong Zhang for helpful discussions and suggestions related to this paper. This work is financially supported in part by the National Key R&D Program of China (Grants No. 2021YFA1601500 and No. 2023YFA1606401), the Strategic Priority Research Program of Chinese Academy of Sciences (Grant No. XDB34000000), the Youth Innovation Promotion Association of the Chinese Academy of Sciences (Grants No. 2022423, No. 2021419, and No. 2019406), and the NSFC (Grants No. 12135017, No. 12121005, No. 12322507, No. 11975280, and No. 11905261).

[1] W. H. G. Lewin, J. Van Paradijs, and R. E. Taam, X-ray bursts, Space Sci. Rev. **62**, 223 (1993).
[2] A. Parikh, J. José, G. Sala, and C. Iliadis, Nucleosynthesis in type I X-ray bursts, Prog. Part. Nucl. Phys. **69**, 225 (2013).
[3] R. H. Cyburt, A. M. Amthor, A. Heger, E. Johnson, L. Keek, Z. Meisel, H. Schatz, and K. Smith, Dependence of X-ray burst models on nuclear reaction rates, Astrophys. J. **830**, 55 (2016).
[4] S. E. Woosley and R. E. Taam, γ-ray bursts from thermonuclear explosions on neutron stars, Nature (London) **263**, 101 (1976).
[5] P. C. Joss, X-ray bursts and neutron-star thermonuclear flashes, Nature (London) **270**, 310 (1977).
[6] M. Y. Fujimoto, T. Hanawa, and S. Miyaji, Shell flashes on accreting neutron stars and X-ray bursts, Astrophys. J. **247**, 267 (1981).
[7] R. K. Wallace and S. E. Woosley, Explosive hydrogen burning, Astrophys. J. Suppl. Ser. **45**, 389 (1981).
[8] L. van Wormer, J. Görres, C. Iliadis, M. Wiescher, and F. K. Thielemann, Reaction rates and reaction sequences in the rp-process, Astrophys. J. **432**, 326 (1994).
[9] H. Schatz, A. Aprahamian, J. Görres, M. Wiescher, T. Rauscher, J. Rembges, F.-K. Thielemann, B. Pfeiffer, P. Möller, K.-L. Kratz, H. Herndl, B. Brown, and H. Rebel, rp-process nucleosynthesis at extreme temperature and density conditions, Phys. Rep. **294**, 167 (1998).
[10] S. E. Woosley, A. Heger, A. Cumming, R. D. Hoffman, J. Pruet, T. Rauscher, J. L. Fisker, H. Schatz, B. A. Brown, and M. Wiescher, Models for type I X-ray bursts with improved nuclear physics, Astrophys. J. Suppl. Ser. **151**, 75 (2004).

[11] J. L. Fisker, H. Schatz, and F.-K. Thielemann, Explosive hydrogen burning during type I X-ray bursts, Astrophys. J. Suppl. Ser. **174**, 261 (2008).

[12] H. Schatz, The importance of nuclear masses in the astrophysical rp-process, Int. J. Mass Spectrom. **251**, 293 (2006).

[13] H. Schatz and W.-J. Ong, Dependence of X-ray burst models on nuclear masses, Astrophys. J. **844**, 139 (2017).

[14] M. Wang, W. Huang, F. Kondev, G. Audi, and S. Naimi, The AME 2020 atomic mass evaluation (II). Tables, graphs and references, Chin. Phys. C **45**, 030003 (2021).

[15] G. M. Fuller, W. A. Fowler, and M. J. Newman, Stellar weak interaction rates for intermediate-mass nuclei. II - A = 21 to A = 60, Astrophys. J. **252**, 715 (1982).

[16] H. Schatz, A. Aprahamian, V. Barnard, L. Bildsten, A. Cumming, M. Ouellette, T. Rauscher, F.-K. Thielemann, and M. Wiescher, End point of the *rp* process on accreting neutron stars, Phys. Rev. Lett. **86**, 3471 (2001).

[17] V.-V. Elomaa, G. K. Vorobjev, A. Kankainen, L. Batist, S. Eliseev, T. Eronen, J. Hakala, A. Jokinen, I. D. Moore, Y. N. Novikov, H. Penttilä, A. Popov, S. Rahaman, J. Rissanen, A. Saastamoinen, H. Schatz, D. M. Seliverstov, C. Weber, and J. Äystö, Quenching of the SnSbTe cycle in the *rp* process, Phys. Rev. Lett. **102**, 252501 (2009).

[18] O. Forstner, H. Herndl, H. Oberhummer, H. Schatz, and B. A. Brown, Thermonuclear reaction rate of ^{56}Ni$(p,\gamma)^{57}$Cu and ^{57}Cu$(p,\gamma)^{58}$Zn, Phys. Rev. C **64**, 045801 (2001).

[19] NucNet Tools, https://sourceforge.net/p/nucnet-projects/wiki/Home/.

[20] C. Langer, F. Montes, A. Aprahamian, D. W. Bardayan, D. Bazin, B. A. Brown, J. Browne, H. Crawford, R. H. Cyburt, C. Domingo-Pardo, A. Gade, S. George, P. Hosmer, L. Keek, A. Kontos, I. Y. Lee, A. Lemasson, E. Lunderberg, Y. Maeda, M. Matos *et al.*, Determining the *rp*-process flow through ^{56}Ni: Resonances in ^{57}Cu$(p,\gamma)^{58}$Zn identified with Gretina, Phys. Rev. Lett. **113**, 032502 (2014).

[21] Y. H. Lam, N. Lu, A. Heger, A. M. Jacobs, N. A. Smirnova, T. K. Nieto, Z. Johnston, and S. Kubono, The regulated Nicu cycles with the new ^{57}Cu$(p,\gamma)^{58}$ Zn reaction rate and its influence on type I X-ray bursts: the GS 1826–24 clocked burster, Astrophys. J. **929**, 73 (2022).

[22] D. Kahl, P. J. Woods, T. Poxon-Pearson, F. M. Nunes, B. A. Brown, H. Schatz, T. Baumann, D. Bazin, J. A. Belarge, P. C. Bender, B. Elman, A. Estrade, A. Gade, A. Kankainen, C. Lederer-Woods, S. Lipschutz, B. Longfellow, S. J. Lonsdale, E. Lunderberg, F. Montes *et al.*, Single-particle shell strengths near the doubly magic nucleus ^{56}Ni and the ^{56}Ni$(p,\gamma)^{5}$Cu reaction rate in explosive astrophysical burning, Phys. Lett. B **797**, 134803 (2019).

[23] K. K. Seth, S. Iversen, M. Kaletka, D. Barlow, A. Saha, and R. Soundranayagam, Mass of proton-rich ^{58}Zn by pion double charge exchange, Phys. Lett. B **173**, 397 (1986).

[24] M. Wang, Y. H. Zhang, X. Zhou, X. H. Zhou, H. S. Xu, M. L. Liu, J. G. Li, Y. F. Niu, W. J. Huang, Q. Yuan, S. Zhang, F. R. Xu, Y. A. Litvinov, K. Blaum, Z. Meisel, R. F. Casten, R. B. Cakirli, R. J. Chen, H. Y. Deng, C. Y. Fu *et al.*, Mass measurement of upper fp-shell $N = Z - 2$ and $N = Z - 1$ nuclei and the importance of three-nucleon force along the $N = Z$ line, Phys. Rev. Lett. **130**, 192501 (2023).

[25] M. Wang, M. Zhang, X. Zhou, Y. H. Zhang, Y. A. Litvinov, H. S. Xu, R. J. Chen, H. Y. Deng, C. Y. Fu, W. W. Ge, H. F. Li, T. Liao, S. A. Litvinov, P. Shuai, J. Y. Shi, M. Si, R. S. Sidhu, Y. N. Song, M. Z. Sun, S. Suzuki *et al.*, $B\rho$-defined isochronous mass spectrometry: An approach for high-precision mass measurements of short-lived nuclei, Phys. Rev. C **106**, L051301 (2022).

[26] M. Zhang, X. Zhou, M. Wang, Y. H. Zhang, Y. A. Litvinov, H. S. Xu, R. J. Chen, H. Y. Deng, C. Y. Fu, W. W. Ge, H. F. Li, T. Liao, S. A. Litvinov, P. Shuai, J. Y. Shi, R. S. Sidhu, Y. N. Song, M. Z. Sun, S. Suzuki, Q. Wang *et al.*, $B\rho$-defined isochronous mass spectrometry and mass measurements of ^{58}Ni fragments, Eur. Phys. J. A **59**, 27 (2023).

[27] J. Xia, W. Zhan, B. Wei, Y. Yuan, M. Song, W. Zhang, X. Yang, P. Yuan, D. Gao, H. Zhao, X. Yang, G. Xiao, K. Man, J. Dang, X. Cai, Y. Wang, J. Tang, W. Qiao, Y. Rao, Y. He *et al.*, The heavy ion cooler-storage-ring project HIRFL-CSR at Lanzhou, Nucl. Instrum. Methods Phys. Res. A **488**, 11 (2002).

[28] W. Zhan, H. Xu, G. Xiao, J. Xia, H. Zhao, and Y. Yuan, Progress in HIRFL-CSR, Nucl. Phys. A **834**, 694c (2010).

[29] Y. Yuan, J. Yang, J. Xia, P. Yuan, W. Qiao, D. Gao, G. Xiao, H. Zhao, H. Xu, M. Song, X. Yang, X. Cai, L. Ma, X. Yang, K. Man, Y. He, Z. Zhou, J. Zhang, Z. Xu, Y. Liu *et al.*, Status of the HIRFL-CSR complex, Nucl. Instrum. Methods Phys. Res. B **317**, 214 (2013).

[30] H. Herndl, J. Görres, M. Wiescher, B. A. Brown, and L. Van Wormer, Proton capture reaction rates in the *rp* process, Phys. Rev. C **52**, 1078 (1995).

[31] N. Shimizu, T. Mizusaki, Y. Utsuno, and Y. Tsunoda, Thick-restart block Lanczos method for large-scale shell-model calculations, Comput. Phys. Commun. **244**, 372 (2019).

[32] M. Honma, T. Otsuka, B. A. Brown, and T. Mizusaki, Shell-model description of neutron-rich pf-shell nuclei with a new effective interaction GXPF 1, Eur. Phys. J. A **25**, 499 (2005).

[33] R. H. Cyburt, A. M. Amthor, R. Ferguson, Z. Meisel, K. Smith, S. Warren, A. Heger, R. D. Hoffman, T. Rauscher, A. Sakharuk, H. Schatz, F. K. Thielemann, and M. Wiescher, The JINA Reaclib database: Its recent updates and impact on type-I X-ray bursts, Astrophys. J. Suppl. Ser. **189**, 240 (2010).

[34] JINA REACLIB Database, https://reaclib.jinaweb.org/.

[35] C. Iliadis, Thermonuclear Reactions, in *Nuclear Physics of Stars* (John Wiley & Sons, Ltd, New York, 2015), Chap. 3, pp. 139–206.

[36] A. Parikh, J. José, C. Iliadis, F. Moreno, and T. Rauscher, Impact of uncertainties in reaction q values on nucleosynthesis in type I X-ray bursts, Phys. Rev. C **79**, 045802 (2009).

[37] T. Rauscher and F.-K. Thielemann, Astrophysical reaction rates from statistical model calculations, At. Data Nucl. Data Tables **75**, 1 (2000).